Influence of the Composite Action for EBFs with Long Dissipative Links

Mihai Șenilă[1)], Florea Dinu[2,3)], Calin Neagu[4,5)], Andreea Onea[6,7*)], Ioan Petran[8)]

[1)] Technical University of Cluj-Napoca, 400114, Cluj-Napoca, Romania, e-mail: roland.senila@dst.utcluj.ro, ioan.petran@dst.utcluj.ro, 0009-0007-9460-1526
[2)] Politehnica University Timisoara, 300006, Timisoara, Romania, e-mail: florea.dinu@upt.ro, 0000-0002-7192-6973
[3)] Romanian Academy, Timisoara Branch, 300223, Timisoara, Romania, e-mail: florea.dinu@upt.ro, 0000-0002-7192-6973
[4)] Politehnica University Timisoara, 300006, Timisoara, Romania, e-mail: calin.neagu@upt.ro, 0000-0002-6828-1043
[5)] Romanian Academy, Timisoara Branch, 300223, Timisoara, Romania, e-mail: calin.neagu@upt.ro, 0000-0002-6828-1043
[6*)] Technical University of Cluj-Napoca, 400114, Cluj-Napoca, Romania, e-mail: andreea.onea@campus.utcluj.ro, 0009-0001-1415-3839
[7*)] Politehnica University Timisoara, 300006, Timisoara, Romania, e-mail: andreea.onea@campus.utcluj.ro, 0009-0001-1415-3839
[8)] Technical University of Cluj-Napoca, 400114, Cluj-Napoca, Romania, e-mail: ioan.petran@dst.utcluj.ro, 0000-0003-2387-8994

https://doi.org/10.29227/IM-2025-02-02-046

Submission date: *2025-05-29* | Review date: *2025-06-24*

Abstract

Steel frame structures are widely used in various types of constructions. With much longer experience and tradition in practice, the Moment Resisting Frames (MRF) and Concentrically Braced Frames (CBF) were the predominant lateral load resisting systems for many decades, thanks to their architectural versatility and high ductility (MRF) or high lateral stiffness (CBF), respectively. On the other hand, the much newer Eccentrically Braced Frame EBF system, may be a viable alternative, thanks to an appropriate combination of stiffness and ductility. In this study, we investigated the effect of composite action between the link beam and the concrete slab on the monotonic and cyclic response of EBFs with long links. The results indicated an increase of initial stiffness and yield resistance of the system, but a small impact on the ductility. Also, the simple detachment of the concrete slab from the beam by the lack of shear studs does not fully eliminate the composite action in links, which may affect both the local and global behavior.

Keywords: eccentrically braced frame; composite action; cyclic load; long link; experimental testing

1. Introduction

Steel frame structures are widely used in various types of constructions. Although structural steel frame configurations include various shapes and typologies, when lateral force resistance is of concern three systems are of interest, namely Moment Resisting Frames (MRF), Concentrically Braced Frames (CBF), and Eccentrically Braced Frames (EBF). With much longer experience and tradition in practice, the first two systems benefit from architectural versatility and high ductility (MRF) and high lateral stiffness (CBF), respectively. On the other hand, EBFs, which are relatively newer systems, first introduced in the 1970s, are known for their appropriate combination of stiffness and ductility characteristics [1], [2]. The recognition of EBFs as high ductility systems followed intensive research developed mostly in US [3], [4] and Japan [5]. In fact, the first developments of EBFs, called "Y-braced frames" in [5], now most commonly known as EBF with vertical link, looked for a compromise between the ductility (of MRFs) and stiffness (of CBFs) by introducing a stub (i.e., link) of different sizes and lengths. Later on, the interest in EBF systems led to the introduction of code procedures for the design of new buildings in other codes. Thus, EN 1998-1 [6] lists EBFs among the structures capable of dissipating large energy and distinguishes between short, intermediate, and long links in function of the shear and flexural characteristics, and respectively between the energy dissipation mechanisms. For such elements, EN 1998-1 [6] introduces a set of rules for the design of frames with eccentric bracings, with or without composite action.

Following the early application rules and the first practical applications, eccentric link-based systems have experienced continuous developments. In a review of research on steel EBFs [7], the impact on local and global behavior of several components, like the effect of axial force, interaction with the concrete slab, loading history, wall slenderness, link detailing, and lateral bracing, has been discussed.

An experimental test campaign performed on real-scale one story/one bay frames with horizontal and vertical links by [8] *Caprili et al.* (2018). The results were the basis of the elaboration of a simple semi-analytical model for the quick representation of the cyclic behaviour of shear links. Y-shaped eccentrically braced frames made from high strength steel HSS were experimentally investigated and reported in [9]. The results showed an ultimate rotation capacity of 0.06 rad, lower than rotation angle limitation of 0.08 rad for the shear link [6], but it is still considered a safe system with reliable hysteretic behaviours and seismic performance. Using HSS in the members of an EBF except the link, where lower nominal yield strength is used, the energy dissipation and improved seismic performance may be enhanced [10].

Composite action between the beams of the seismic force-resisting system (SFRS) and the concrete slab is a general problem when ductility during seismic response is of interest, not only for EBFs but other frame typologies, e.g., MRFs. To neglect the composite action (either in MRF or EBF), the beams (or links) should be disconnected over the dissipative zones. However, by eliminating the shear connectors in dissipative zones, the results reported in [11], [12] showed that the composite action is not fully eliminated. Short, shear yielding links are preferred in eccentrically braced frames (EBFs) because of their demonstrated excellent strength, stiffness, and energy-dissipation capacity. Longer flexural yielding links, however, can offer important architectural [13]. Also, the experimental results reported in [13] and [14] pointed out that long links, i.e., D-braced EBF, should not be attached to

columns. In case of eccentrically braced frames with long links, the results reported in [15], [16], [17] pointed out the use of composite action between the links and the concrete slab enhances the seismic response if compared with bare steel systems.

Although it is not explicitly classified, ANSI/AISC 341-16 [18] provides limitations of the link rotation angle for three ranges of the link length which is proportional to the ratio between the plastic bending moment and plastic shear strength.

Traditional prescriptive seismic provisions for new buildings principally concentrate on the Life Safety objective. Little consideration is given to either the actual performance of individual buildings or the economic loss and occupancy interruption that may occur after an earthquake [19]. Therefore, specific topics emerged in the construction industry, e.g., seismic resilience. While resilience can have several components, two are of importance when structural systems are envisaged, i.e., the capacity to resist the hazard, or robustness, and the ability to recover from the hazard, which means lower damage (and costs), and lower duration of intervention.

To make the constructions more seismically resilient, the design provisions and construction techniques should favor the use low-damage/replaceable techniques [20], [21], [22], [23]:

i. low-damage structures: limit damage in structures so that they do not need to be replaced immediately after a major loading event.
ii. replaceable technology: damage to occur in a few locations (easily accessible if possible) where replacement/repairing of damaged components may easily be conducted.

The study presented in the paper investigated the monotonic and cyclic response of EBFs with long links considering three different configurations, i.e., bare steel link, composite steel beam with concrete slab disconnected from the links, and composite steel beam with concrete slab connected to the links with shear connectors.

2. Experimental program

An experimental program was carried out to investigate the monotonic and cyclic performance of EBF systems. Three systems have been considered, i.e., bare steel link, composite steel beam with concrete slab disconnected from the links, and composite steel beam with concrete slab connected to the links with shear connectors. The specimens were isolated from a single reference structural configuration, which is a 5 story, 3 bays, and 3 spans structure. The outer bays and spans have 6.0 m, while the inner EBF has 4.5 m. The height is 3.5 m for the first story and 3.0 m for the upper floors. The geometry of the reference structure is presented in Fig. 1. The reference structure has been designed for persistent and seismic design situations, using the following load cases:

- Permanent load: G = 4.5 kN/m^2
- Live load: Q = 3.0 kN/m^2
- Snow load: S = 1.6 kN/m^2
- The seismic action parameters: control period T_c = 1.6 s, peak horizontal ground acceleration a_g = 0.3 g, and behaviour factor q = 6.0. The design has been done considering Eurocode provisions.

The final configuration of the reference eccentrically braced frame intended to be tested is presented in Fig. 2.

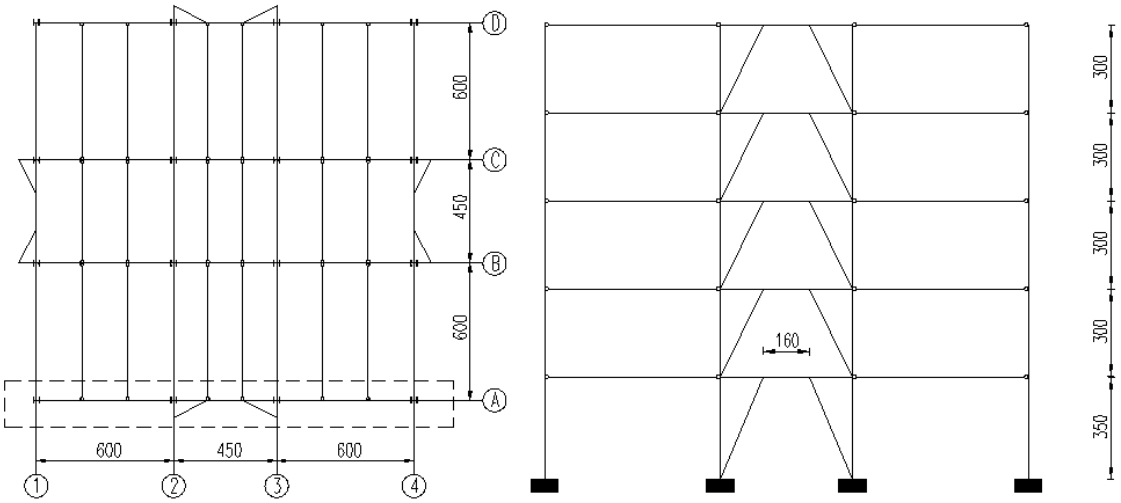

Fig. 1. Current floor plan and transversal frame of the reference structure

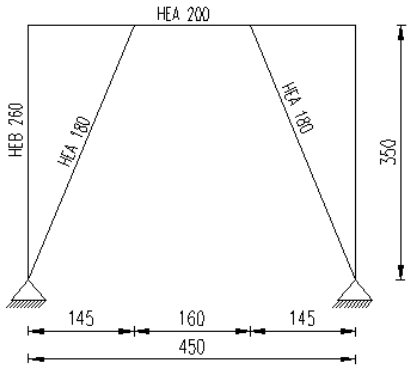

Fig. 2. Geometry of the EBF configuration proposed for experimental testing (in cm)

The columns and braces are non-dissipative members and were designed with sufficient overstrength to allow the development of cyclic yielding in the dissipative links [6]. Therefore, they were reused during the successive tests, and only the steel beams, including the link, were replaced for each test. Fig. 3 to Fig. 6 present the geometry, cross-sections and details for beams, links and concrete slab (for specimens with composite beams, only).

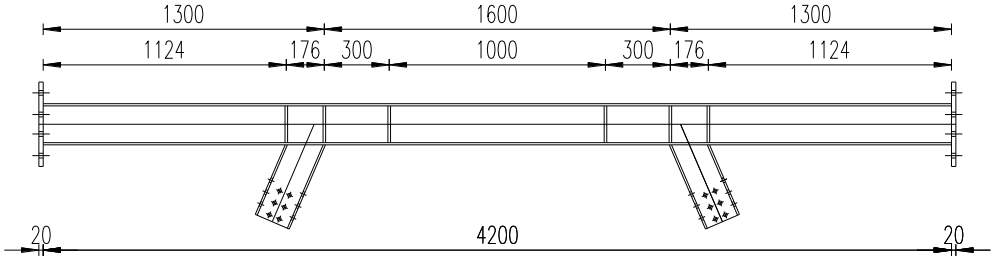

Fig. 3. Bare steel beam and link (in mm)

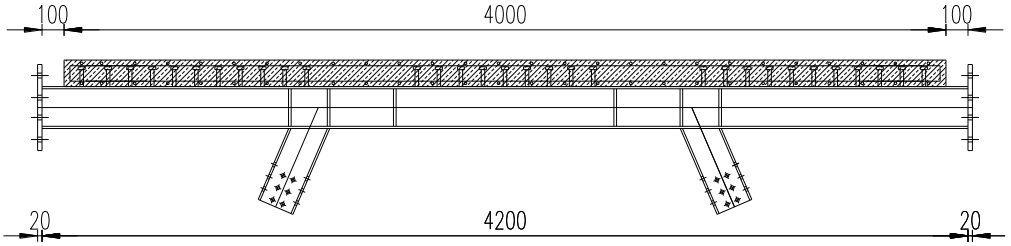

Fig. 4. Composite beam and link partially connected to the concrete slab (in mm)

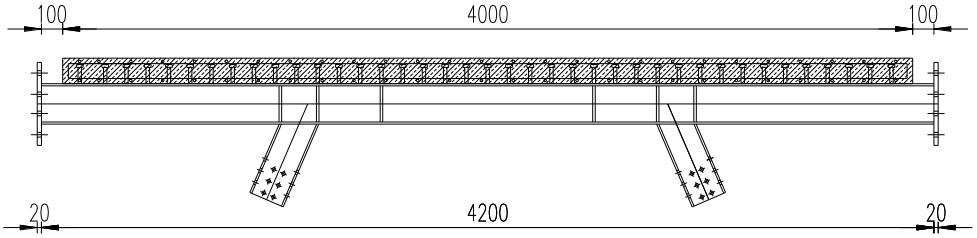

Fig. 5. Composite beam and link fully connected to the concrete slab (in mm)

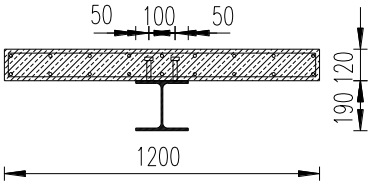

Fig. 6. Composite beam cross-section (in mm)

Nelson shear studs with 19 mm diameter were welded to the top flange on two rows to obtain the interaction between the steel beam/link and the concrete slab. A fully composite connection was considered for the action of the composite beam. The height of the slab was 120 mm, and the connectors were 90 mm long. C25/30 class properties were used for the concrete slab. The slab was reinforced with 12 mm bars made from a steel with nominal yield strength of 355 N/mm^2. The rebars were positioned on both directions at 150 mm intervals. The spacing between connectors was 80 mm, with a 480 mm gap along the potential plastic zone of the links.

For each type of specimens, two loading protocols were considered, i.e., monotonic and cyclic. The monotonic tests have been employed for the determination of the yield force (F_y) and the corresponding displacement (e_y) that are further employed in the cyclic tests. The yield force and the corresponding displacement were obtained considering the intersection of the elastic rigidity and the tangent of the tenth percent of the initial rigidity to the force displacement curve, see Fig. 7a. Considering the loading protocol recommended by European Conventions for Constructional Steelwork [24], one cycle for $e_y/4$, 2 $e_y/4$, 3 $e_y/4$, e_y and three cycles for each even (2, 4, 6….) e_y (Fig. 7b) were performed until the reduction of the applied force by 20%. The name of each test configuration is given in Tab. 1.

The joints between beams and columns were designed as rigid and constructed using extended end plate bolted connections, using 8 M20 class 10.9 bolts and 24 mm end plates, see Fig. 8a. Braces were spliced using bolted gusset plate connections. The pinned column base is presented in Fig. 8b. Fig. 9 shows photos during the fabrication of composite beam specimens.

The loading was applied quasi-statically in displacement control using displacement control and two 1200 kN hydraulic jacks placed at the beam level and connected to a reaction wall, see Fig. 10 . For the cyclic tests, each jack was engaged alternatively, for the two directions of the loading.

The mechanical properties of steel from beams, links, columns, braces, as well as reinforcing bars were evaluated using standard tensile coupon tests, see Tab. 2. Tab. 3 shows the characteristic values for the concrete material obtained using 150 mm cubes cured for 28 days.

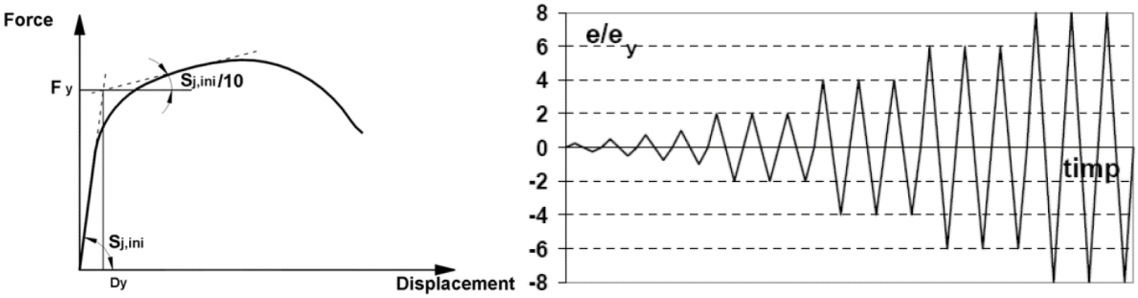

a) b)

Fig. 7. Loading protocols: a) determination of F_y and e_y; b) cyclic loading protocol

Tab. 1. The experimental program details 1.

Specimen	Beam type	Loading protocol	Connectors on link
BS-M	Steel	Monotonic	-
BS-C	Steel	Cyclic	-
PC-M	Composite	Monotonic	Partial
PC-C	Composite	Cyclic	Partial
FC-M	Composite	Monotonic	Total
FC-C	Composite	Cyclic	Total

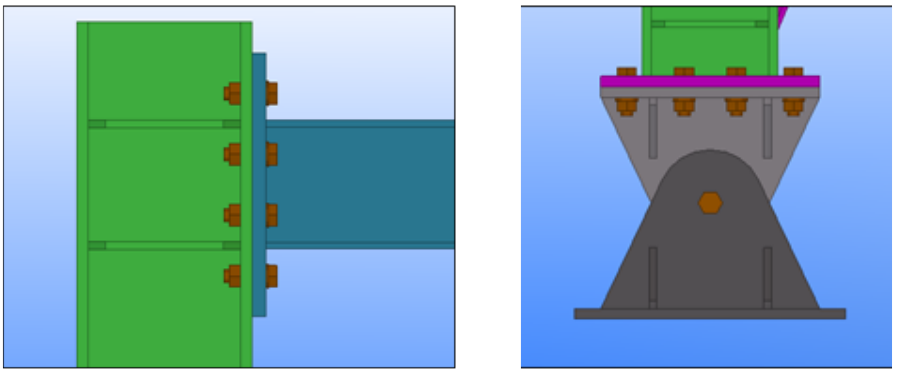

a) b)

Fig. 8. a) Extended end plate beam-column connections, b) pinned column base connection

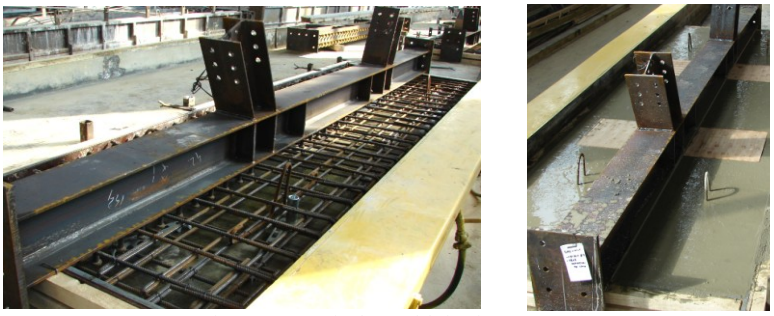

Fig. 9. Composite beam fabrication process

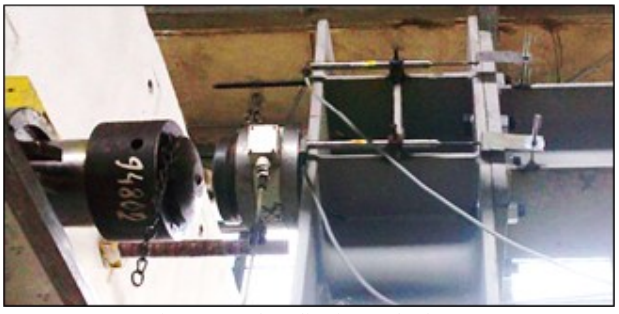

Fig. 10. Load application to the frame

Tab. 2. Steel properties

Element	Section	Part	Nominal material	Yield strength, f_y N/mm^2	Tensile strength, f_u N/mm^2
Beam	HEA200	Web Flange	S235	277 285	419 403
Column	HEB 260	Web Flange	S355	283 283	440 440
Bracing	HEA180	Web Flange	S355	309 288	409 426
Rebar	Ø12	-	S355	367	562

Tab. 3. Concrete properties.

Density	2351 kg/m^3
Compressive strength at mould removal	21.9 N/mm^2
Compressive strength at delivery	32.30 N/mm^2
Compressive strength at 28 days	37.16 N/mm^2

3. Experimental results

For each test, the top displacement was recorded at the load application point, corrected with the displacements caused by the connection's tolerances recorded at the base of the frame. The cyclic tests were stopped when the maximum force in a cycle decreased by more than 30% compared with the peak force.

3.1 Bare steel frame, BS

The response of the EBF specimen with bare steel link under monotonic loading confirmed the expectations, as the failure occurred by the excessive plasticization in the dissipative zones (see Fig. 11), with some out of plane due to the rather large flexibility of the out-of-plane restraining structure. The force-displacement curve is presented in Fig. 12a, with a maximum force of 204 kN at a corresponding displacement of 44 mm. When the force decreased to 193 kN, the test was stopped; the corresponding ultimate displacement was 53. The link rotation at the peak force was 14 mrad, and reached 20 mrad at ultimate state, see Fig. 12b. A reference yield displacement e_y of 14 mm was determined, which was further used to configure the cyclic loading protocol.

The force-displacement and moment rotation curves in the cyclic test are presented in Fig. 13. The response of the specimen to cyclic loads satisfies the code requirements, with an ultimate rotation capacity of 0.02 rad. Some of the out-of-plane deformations of the frame have been also recorded at failure.

Fig. 11. Failure of the link for BS-M

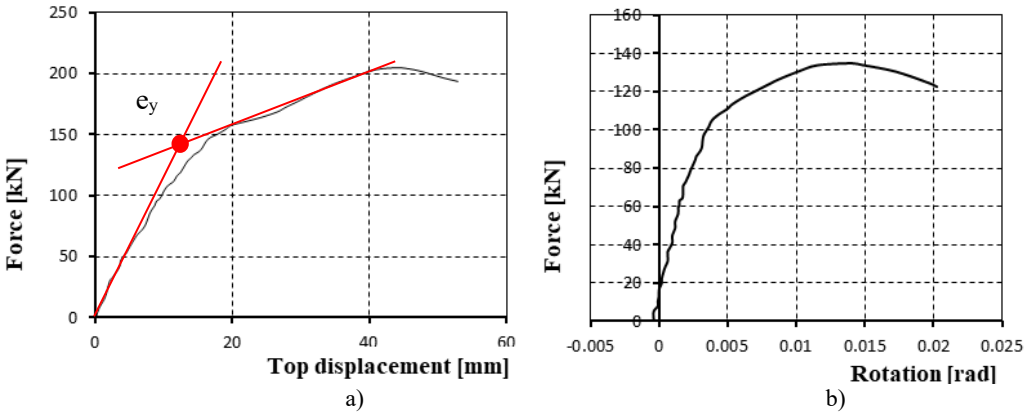

Fig. 12. BS-M: a) Force-displacement curve and yielding point definition e_y; b) Moment-rotation curve

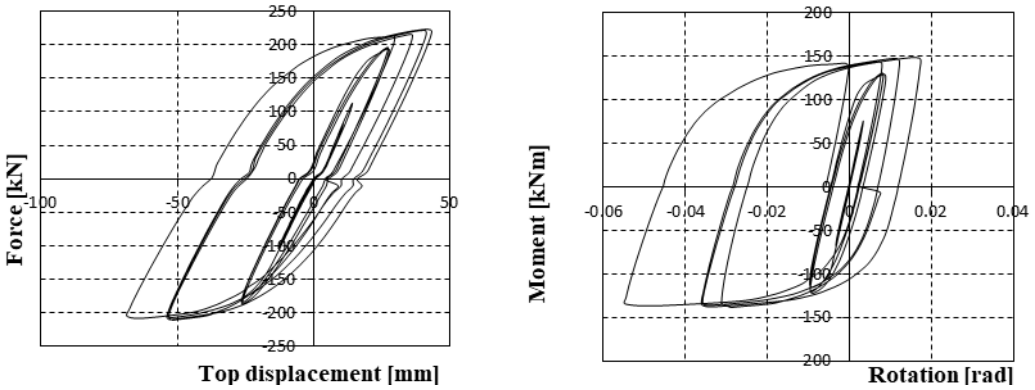

a) b)

Fig. 13. BS-C a) Force-displacement curve b) Moment-rotation curve

3.2 Partially composite specimens, PC

To neglect the composite action in links, the steel beam and concrete slab were disconnected over the dissipative zones, see Fig. 4. The failure of the specimen during monotonic test occurred by the detachment of the concrete slab and the pull-out of the connectors. For the monotonic test, the connector pull-out occurred in the compressed part of the concrete slab. Fig. 14 shows also that the plasticization of the compressed flange of the link, which is more visible on the right side of the frame, where the bottom flange is in compression. Despite there are no connectors along the link ends (the potential dissipative areas), it is observed the beneficial effect of the concrete slab in the stabilization of the top flange where compressive stresses develop. Although the configuration of the restraining out-of-plane system was similar to the bare steel structure, the concrete slab prevented the out-of-plane displacements of the EBF noticed in the case of BS specimen. The maximum applied force recorded 354 kN at a displacement of 80 mm. When the force dropped to 300 kN, the test was stopped; the corresponding displacement measured 115 mm, see Fig. 15a. As may be observed in Fig. 15b, the specimen exhibits a high dissipative capacity as plastic deformations develop at both link ends. The ultimate plastic link rotation, θ_p, at each end was approximately 41 mrad. The yield displacement from monotonic test amounted 18 mm, but for consistency parameters, a reference displacement of 14 mm was considered for the cyclic test, same as in case of BS-C specimen.

Fig. 14. Failure of the link for PC-M

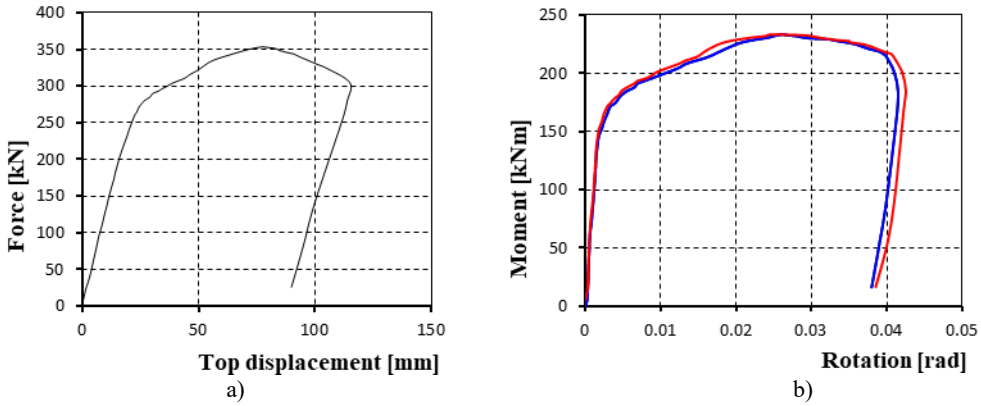

a) b)

Fig. 15. Force-displacement curve (a) and moment-rotation curve at left end link (blue) and right end link (red) (b), test PC-M

The maximum force in the cyclic loading test was obtained in the first cycle of $4e_y$ amplitude, when the peak force recorded 367 kN, and the corresponding displacement 55 mm, see Fig. 16. The test was stopped in the second cycle of the loading corresponding to an amplitude of 8ey, when the connection between the beam and the slab was severely reduced and the behavior of the partially composite EBF was similar to that of bare steel EBF. The deformations of the top flange of the link within the link

ends were reduced until the detachment from the concrete slab. After this point, local buckling of the top flange developed, thus contributing to the plastic deformation capacity, see Fig. 17. The moment-rotation curves obtained for each side of the link are presented in Fig. 18, showing relatively similar characteristics both on the negative and positive bending moment branches.

The link rotation is consistent with the code requirements in terms of acceptance criteria (i.e., plastic rotation capacity), i.e., 20 mrad. For the plastic rotation considered by the FEMA 356 [25], the recorded rotation exceed the value computed for the HEA200 steel section for long links. By observing the moment-rotation curves and failure mode presented Fig. 17, one may say that the concrete slab has a restraining effect on the top flange, and the bottom flange develops larger plastic deformations.

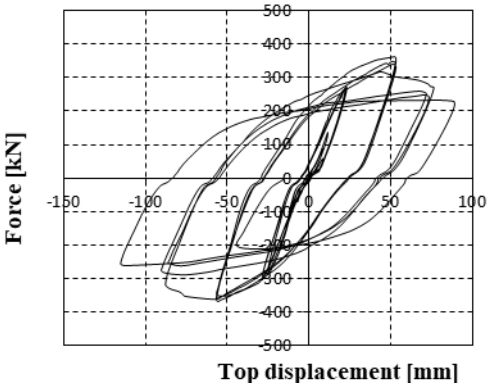

Fig. 16. Force-displacement curve for PC-C

a) b)

Fig. 17. Failure of the link for PC-C

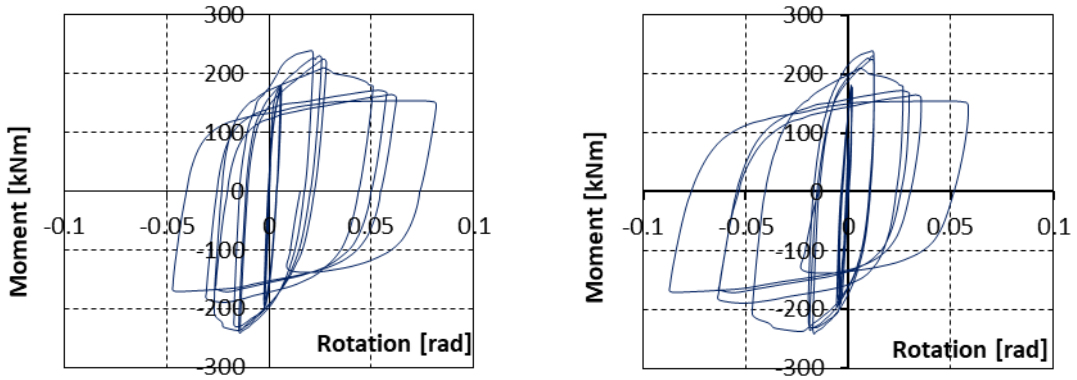

a) b)

Fig. 18. Moment-rotation curve for PC-C: a) left side; b) right side

3.3 Fully composite specimens, FC

As expected, for the monotonic test, plastic deformations occurred at the ends of the link together with the buckling of the flange, see Fig. 19. In the final stage of the failure, a detachment of the slab was observed due to the crushing of the concrete near the left-hand side link end. The force displacement curve presented in Fig. 20a indicates a good deformation capacity, with a significant elastic capacity, but also a consistent plastic one. The maximum force recorded 376 kN, at a corresponding displacement of 62 mm. At failure, the force dropped to 355 kN, at a corresponding ultimate displacement of 118 mm. The moment rotation curves calculated for both link ends show a ductile response of the EBF, with ultimate rotations in excess of 43 mrad (for left end) and 48 mrad for right end, see Fig. 20b.

Fig. 19. Failure of the link for FC-M

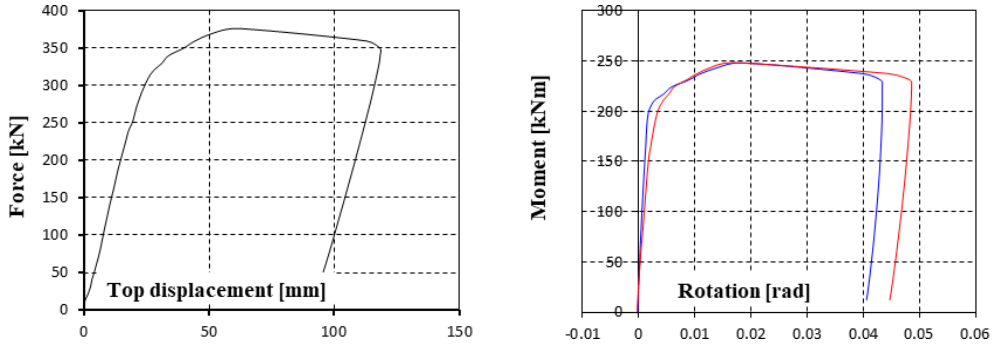

Fig. 20. Force-displacement curve (a) and moment-rotation curve at left end link (blue) and right end link (red) (b), test FC-M

For the cyclic test, the reference yield displacement, e_y, has been considered 14 mm, similar to BS and PC tests. The failure occurred due to the loss of the connection between the link beam and the slab as the connectors were pulled out of concrete. Fig. 21 shows the deformations of the flanges before the connectors pull out, while Fig. 22 the large deformations at the end of the links after the composite action is partially lost. The maximum force was obtained in the first cycle of $4\times e_y$ amplitude, at a force of 405 kN and a displacement of 67 mm, see Fig. 23. Stable hysteretic curves were obtained up to the third cycle of the 6ey amplitude. From this point on, an important increase in displacement was recorded from 86 mm to 104 mm, but with a very small decrease in the force. The moment rotation curves for both dissipative link ends are presented in Fig. 24. The link rotation for the EBF system with fully composite links is consistent with the code requirements in terms of acceptance criteria (plastic rotation capacity), i.e., 20 mrad.

Similar to the partial composite EBF, the plastic deformations increased significantly only after the connectors were pull-out. By comparing the two moment rotation curves (i.e., PC-C and FC-C) (see Fig. 25), it may be seen the plastic deformations of the top flange are lower than the plastic deformations of the bottom flange, which is not constrained by the concrete slab.

Fig. 21. Deformations in the link FC-C before detachment of the slab

Fig. 22. Failure of the link for FC-C, with the detachment of the slab

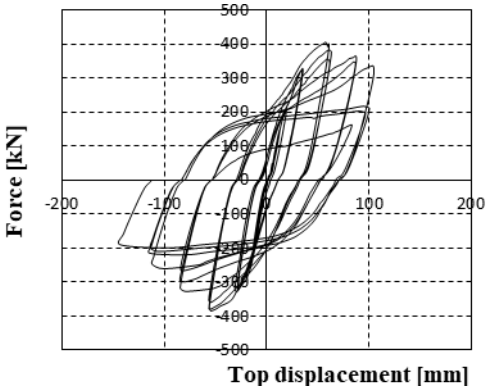

Fig. 23. Force-displacement cyclic curve for FC-C

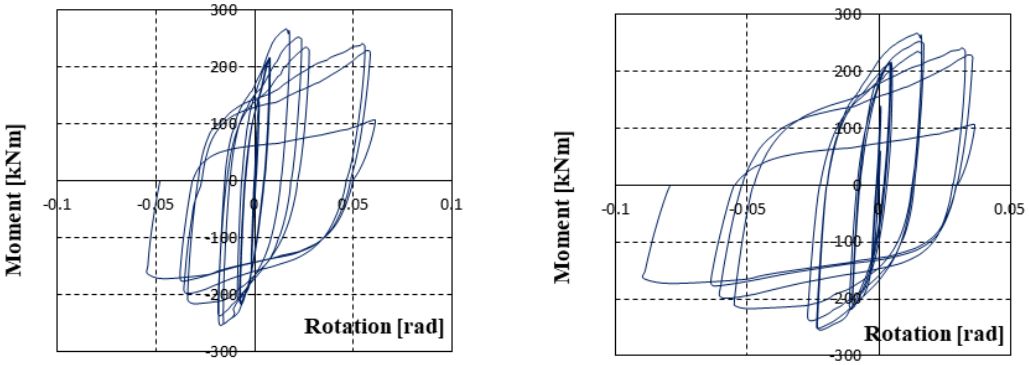

a) b)

Fig. 24. Moment-rotation curve for FC-C: a) left side; b) right side

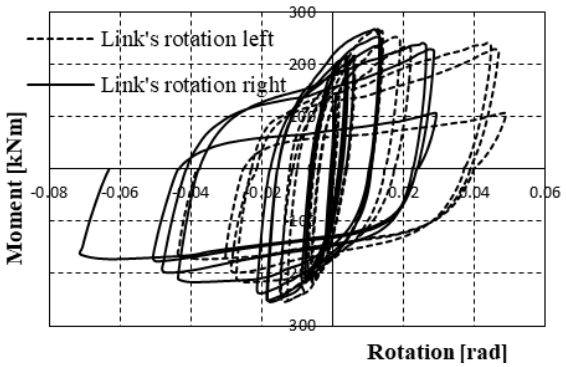

Fig. 25. Moment-rotation curve for FC-C

The results of the experimental tests are summarized in Tab. 4. The data refers to the maximum forces (F_{max}), maximum bending moment on the link ($M_{max,link}$), displacement corresponding to the maximum force (ΔF_{max}), maximum displacement of the frame (Δ_{max}), plastic rotations of the link corresponding to the maximum moments ($\phi_{M,max}$) and maximum plastic rotations (ϕ_{max}).

For the monotonic loading protocol, an increase of more than 70% was achieved for the composite systems with links either partially or fully attached to the concrete slab. Also, the displacements at maximum forces and the ultimate displacements show significant increases (see Fig. 26).

When the two systems with composite beams are compared, it may be seen there is a slight increase of the maximum force for FC frames. Although a significant increase of the maximum/ultimate rotation of the link developed for the composite solutions, the two solutions show similar performance.

Tab. 4. Summary of test results

Specimen	F_{max} [kN]	$M_{max,link}$ [kNm]	ΔF_{max} [mm]	Δ_{max} [mm]	ϕ_{Mmax} [mrad]	ϕ_{max} [mrad]
BS-M	204.53	134.9	44	53	14	20
BS-C	224.35	148.1	36	59	11	21
PC-M	354.1	233.7	77	115	26	41
PC-C	367.2	242.3	56	89	18	34
FC-M	376.7	248.6	62	118	18	43
FC-C	404.9	267.2	57	104	11	46

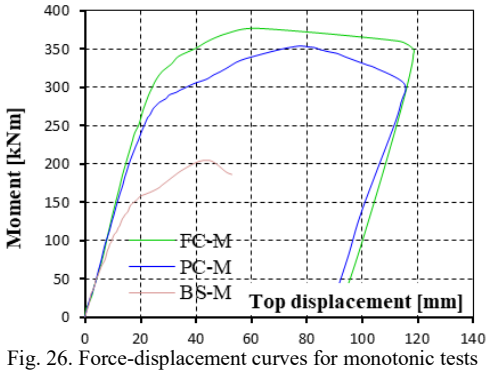

Fig. 26. Force-displacement curves for monotonic tests

When tested under cyclic loading, both systems exhibit a similar response, see Fig. 27. The maximum force recorded for the fully composite system FC-C is approximately 10% larger than the force recorded for the partial composite system PC-C. A similar response is observed for the moment-rotation curve, see Fig. 28. The difference in response in terms of force and mending moment between the two systems keeps the same trend also for cycle 2 and cycle 3, see Fig. 29 and Fig. 30. As may be seen from the moment-rotation curves (Fig. 28 - Fig. 30), an increased stiffness is observed for the fully composite frame FC-C. This is attributed to the continuous presence of the connectors along the links.

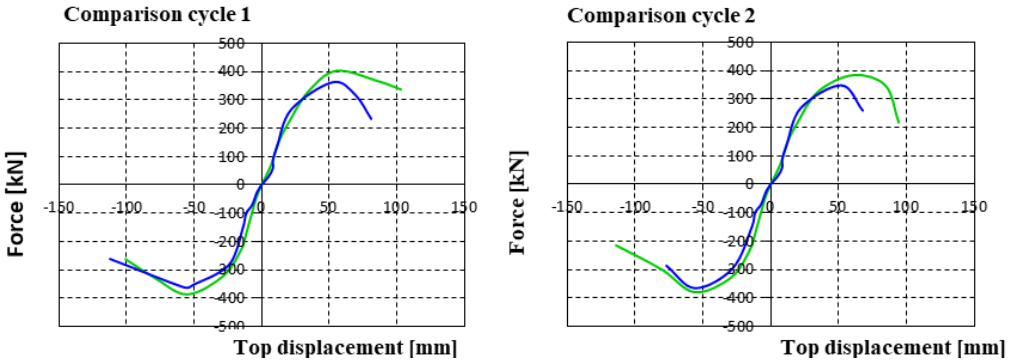

a) b)

Fig. 27. Envelope of the force-displacement curves for cyclic tests on FC-C: a) 1st cycle; b) 2nd cycle

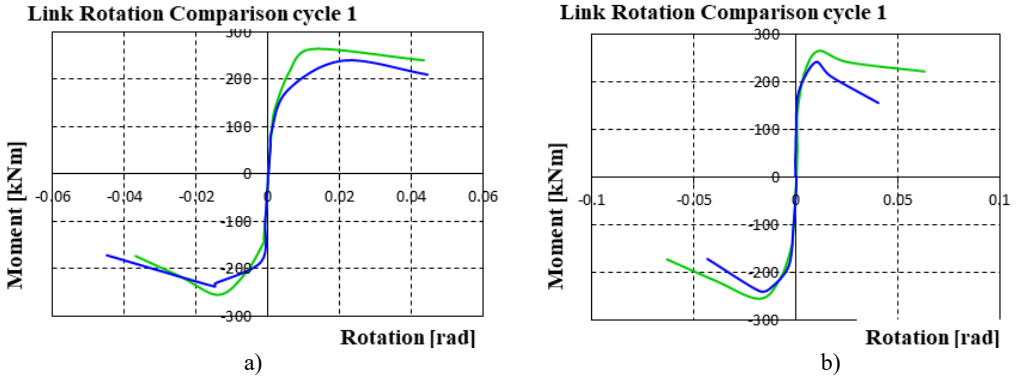

a) b)

Fig. 28. Envelope of the moment-rotation curves for the 1st cycle (FC-C green, PC-C blue): a) link left end, b) link right end

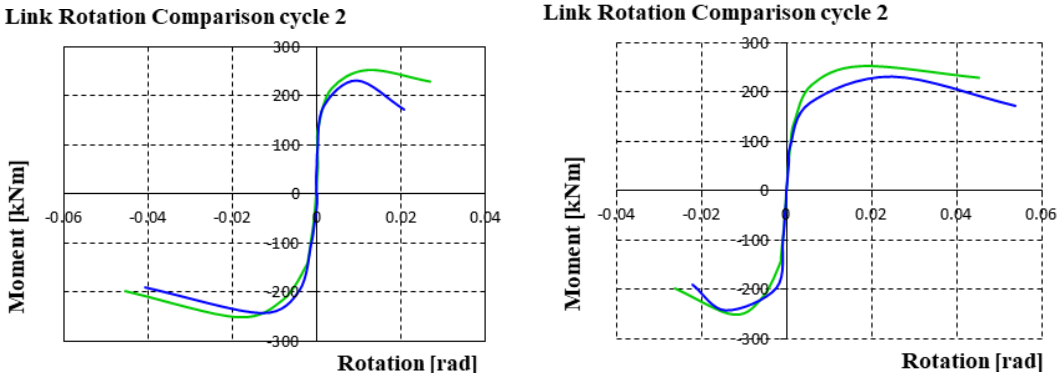

a) b)

Fig. 29. Envelope of the moment-rotation curves for the 2nd cycle (FC-C green, PC-C blue): a) link left end, b) link right end

From the moment-rotation envelope curves obtained in the third cycle, it is observed an asymmetrical response during the positive and negative bending moment. Larger plastic rotations are developed in the area of negative bending moment, because the internal forces are only acting through the rebars of the slab and the free flange of the link is in compression and susceptible to instability effects.

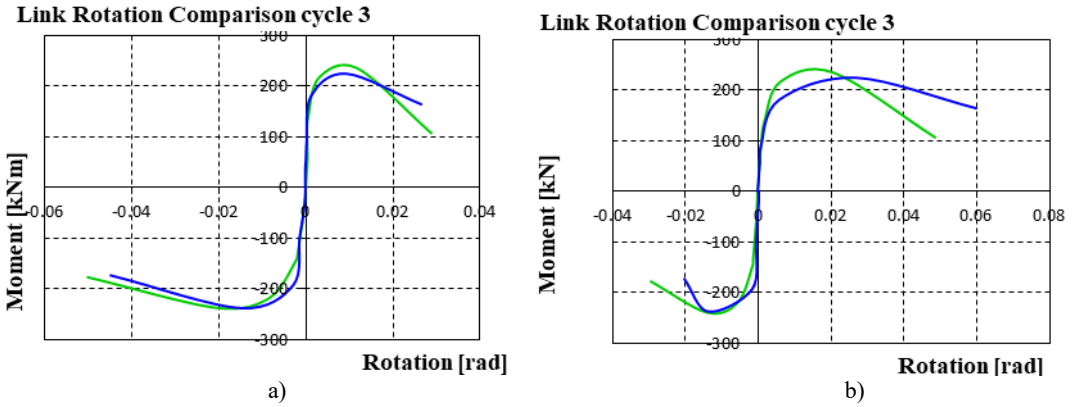

a) b)

Fig. 30. Envelope of the moment-rotation curves for the 3rd cycle (FC-C green, PC-C blue): a) link left end, b) link right end

4. Conclusions

An experimental program was performed to evaluate the monotonic and cyclic response of steel EBFs with long dissipative links. The link beam was realized in three configurations: (1) bare steel, (2) composite steel - concrete beam with connectors on the entire beam exceptive the dissipative zones at the link ends, and (3) composite steel - concrete beam with connectors on the entire beam length, including the dissipative zones at the link ends.

The composite beam structures tested in the experimental program have shown stable energy dissipation characteristics, and good lateral stiffness. No significant differences were observed in the behavior of composite specimens with and without connectors welded on the dissipative zones, and the simple disconnection of the steel beam from the concrete slab over the dissipative zone is not sufficient to ensure a pure bare steel behavior of the element. The resulted behavior is closer to that of a full-composite specimen.

Compared to the bare steel EBF, the composite EBF with long links improves the structural resistance and the initial stiffness, while maintaining the ductile behavior of the system. Due to the influence of the concrete slab, with or without connectors on the dissipative zones, as well as the slippage between the concrete slab and the steel beam, the response of beam-to-column plastic joints have shown unsymmetrical behavior, with larger plastic rotations in the area with negative bending moments, and lower flexural stiffness. the experimental program showed that the behavior of EBFs with long dissipative links designed as composite was adequate considering the minimum requirements criteria stated in seismic design codes.

References

1. American Institute of Steel Construction, “Seismic Provisions for Structural Steel Buildings ANSI/AISC 341-16.” 2016. Accessed: Jan. 29, 2020. [Online]. Available: https://www.aisc.org/Specification-for-Structural-Steel-Buildings-ANSIAISC-360-16
2. E. Hines and C. Jacob, “Eccentric Braced Frame System Performance,” *Structures Congress 2010*, May 2010, doi: 10.1061/41130(369)121.
3. Hjelmstad Keith D. and Popov Egor P., “Cyclic Behavior and Design of Link Beams,” *Journal of Structural Engineering*, vol. 109, no. 10, pp. 2387–2403, Oct. 1983, doi: 10.1061/(ASCE)0733-9445(1983)109:10(2387).
4. E. P. Popov, M. D. Engelhardt, and J. M. Ricles, “Eccentrically Braced Frames: U.S. Practice,” *Eng J*, vol. 26, no. 2, pp. 66–80, Jun. 1989, doi: 10.62913/engj.v26i2.516.
5. R. Tanabashi, K. Naneta, and T. Ishida, “On the rigidity and ductility of steel bracing assemblage,” in *Proceedings of the 5th World Conference on Earthquake Engineering*, IAEE Rome, 1974, pp. 834–840.
6. CEN, *EN 1998-1:2004 - Eurocode 8: Design of structures for earthquake resistance - Part 1: General rules, seismic actions and rules for buildings*. 2004.
7. S. Kazemzadeh Azad and C. Topkaya, “A review of research on steel eccentrically braced frames,” *Journal of Constructional Steel Research*, vol. 128, pp. 53–73, Jan. 2017, doi: 10.1016/j.jcsr.2016.07.032.
8. S. Caprili, N. Mussini, and W. Salvatore, “Experimental and numerical assessment of EBF structures with shear links,” *Steel and Composite Structures*, vol. 28, pp. 123–138, Jul. 2018, doi: 10.12989/scs.2018.28.2.123.
9. M. Lian and M. Su, “Seismic performance of high-strength steel fabricated eccentrically braced frame with vertical shear link,” *Journal of Constructional Steel Research*, vol. 137, pp. 262–285, Oct. 2017, doi: 10.1016/j.jcsr.2017.06.022.
10. X. Tian, M. Su, M. Lian, F. Wang, and S. Li, “Seismic behavior of K-shaped eccentrically braced frames with high-strength steel: Shaking table testing and FEM analysis,” *Journal of Constructional Steel Research*, vol. 143, pp. 250–263, Apr. 2018, doi: 10.1016/j.jcsr.2017.12.030.

11. A. Ciutina, D. Dubina, and G. Danku, “Influence of steel-concrete interaction in dissipative zones of frames: I - Experimental study,” *Steel Compos. Struct.*, vol. 15, no. 3, pp. 299–322, Sep. 2013, doi: 10.12989/scs.2013.15.3.299.
12. G. Danku, D. Dubina, and A. Ciutina, “Influence of steel-concrete interaction in dissipative zones of frames: II − Numerical study,” *Steel and Composite Structures*, vol. 15, no. 3, pp. 323–342, Sep. 2013.
13. Engelhardt M. D. and Popov E. P., “Experimental Performance of Long Links in Eccentrically Braced Frames,” *Journal of Structural Engineering*, vol. 118, no. 11, pp. 3067–3088, Nov. 1992, doi: 10.1061/(ASCE)0733-9445(1992)118:11(3067).
14. E. Mohammadrezapour and F. Danesh, “Experimental investigation of bolted link-to-column connections in eccentrically braced frames,” *Journal of Constructional Steel Research*, vol. 147, pp. 236–246, Aug. 2018, doi: 10.1016/j.jcsr.2018.04.009.
15. M. Senila, A. Sigauan, and I. Petran, “Comparison between behavior of steel and composite Eccentrically Braced Frames with long links,” presented at the RECENT PROGRESS IN STEEL AND COMPOSITE STRUCTURES, M. Gizejowski, A. Kozlowski, J. Marcinowski, and J. Ziolko, Eds., 2016, pp. 237–243.
16. M. Senila and I. Petran, “Plastic hinges in steel and composite eccentrically braced frames with long links,” presented at the MODERN TECHNOLOGIES FOR THE 3RD MILLENNIUM, S. Nistor and G. Popoviciu, Eds., 2018, pp. 357–362.
17. S. R. Mihai, P. Ioan, C. Neagu, and F. Dinu, *Numerical Studies on Seismic Response of Steel and Composite Eccentrically Braced Frames*. Porto: Inegi-Inst Engenharia Mecanica E Gestao Industrial, 2018.
18. AISC, “Seismic provisions for structural steel buildings,” American institute of steel construction, ANSI/AISC 341-16, 2010.
19. J. L. Harris III., National Institute of Standards and Technology (U.S.). Physical Measurement Laboratory. Radiation Physics Division., J. L. III. Harris, and M. S. Speicher, *Assessment of fire generation performance-based seismic design methods for new steel buildings : volume 3: eccentrically braced frames*. in NIST Technical Note ; 1863-3. Gaithersburg, MD: U.S. Dept. of Commerce, National Institute of Standards and Technology, 2015.
20. D. Dubina, A. Stratan, and F. Dinu, “Dual high-strength steel eccentrically braced frames with removable links,” *Earthq. Eng. Struct. Dyn.*, vol. 37, no. 15, Art. no. 15, Dec. 2008, doi: 10.1002/eqe.828.
21. D. Dubina and F. Dinu, “Seismic Resilience of Multi-story Dual-Steel Building Frames,” in *Progresses in European Earthquake Engineering and Seismology*, R. Vacareanu and C. Ionescu, Eds., in Springer Proceedings in Earth and Environmental Sciences. , Cham: Springer International Publishing, 2022, pp. 465–472. doi: 10.1007/978-3-031-15104-0_28.
22. A. Chesoan, A. Stratan, and D. Dubina, “Design implementation of re-centring dual eccentrically braced frames with removable links,” *Soil Dynamics and Earthquake Engineering*, vol. 112, pp. 174–184, Sep. 2018, doi: 10.1016/j.soildyn.2018.05.015.
23. A. Ioan *et al.*, “Experimental validation of re-centring capability of eccentrically braced frames with removable links,” *Engineering Structures*, vol. 113, pp. 335–346, Apr. 2016, doi: 10.1016/j.engstruct.2016.01.038.
24. E. ECCS, “Technical Committee 1–Structural Safety and Loadings–Technical Working Group 1.3–Seismic Design Recommended Testing Procedure for Assessing the Behaviour of Structural Steel Elements under Cyclic Loads,” 1986.
25. ASCE, “FEMA 356 Prestandard and Commentary for the Seismic Rehabilitation of Buildings,” 2000.